1 **Genomic analysis of *Staphylococcus aureus* isolates from bacteremia**

2 **reveals genetic features associated with the COVID-19 pandemic**

3 Miquel Sánchez-Osuna[1,2,#], Marc Pedrosa[3], Paula Bierge[1,2], Inmaculada Gómez-Sánchez[1,2],

4 Marina Alguacil-Guillén[4], Mateu Espasa[4], Ivan Erill[5,6], Oriol Gasch[3], Oscar Q. Pich[1,2,#]

5

6 [1]Laboratori de Recerca en Microbiologia i Malalties Infeccioses, Hospital Universitari Parc Taulí, Institut

7 d'Investigació i Innovació Parc Taulí (I3PT-CERCA), Universitat Autònoma de Barcelona, Sabadell (Spain)

8 [2]Institut de Biotecnologia i Biomedicina, Universitat Autònoma de Barcelona, Cerdanyola del

9 Vallès (Spain)

10 [3]Servei de Malalties Infeccioses, Hospital Universitari Parc Taulí, Institut d'Investigació i Innovació Parc

11 Taulí (I3PT-CERCA), Universitat Autònoma de Barcelona, Sabadell (Spain)

12 [4]Servei de Microbiologia, Hospital Universitari Parc Taulí, Institut d'Investigació i Innovació Parc Taulí

13 (I3PT-CERCA), Universitat Autònoma de Barcelona, Sabadell (Spain)

14 [5]Department of Biological Sciences, University of Maryland Baltimore County, Baltimore (USA)

15 [6]Departament d'Enginyeria de la Informació i de les Comunicacions, Universitat Autònoma de Barcelona,

16 Cerdanyola del Vallès (Spain)

17

18 # Address correspondence to Miquel Sánchez-Osuna or Oscar Q. Pich

19 *msanchezo@tauli.cat*, *oquijada@tauli.cat*

20

21 Keywords: *Staphylococcus aureus*, bacteremia, whole-genome sequencing, disease outcome,

22 associations, antibiotic resistance, virulence factors, COVID-19 pandemic

23

ABSTRACT

Genomic analyses of bacterial isolates are necessary to monitor the prevalence of antibiotic resistance genes and virulence determinants. Herein, we provide a comprehensive genomic description of a collection of 339 *Staphylococcus aureus* strains isolated from patients with bacteremia between 2014 and 2022. Nosocomial acquisition accounted for 56.6% of episodes, with vascular catheters being the predominant source of infection (31.8%). Cases of fatality (27.4%), persistent bacteremia (19.5%) and diagnosis of septic emboli (24.2%) were documented. During the COVID-19 pandemic, we observed a 140% increase of the episodes of *S. aureus* bacteremia per year, with a concomitant increase of the cases from nosocomial origin. This prompted us to investigate the existence of genetic features associated with *S. aureus* isolates from the COVID-19 pandemic. While genes conferring resistance to β-lactams (*blaI-blaR-blaZ*), macrolides (*ermA, ermC, ermT, mphC, msrA*) and aminoglycosides (*ant*(4')-Ia, *ant*(9)-Ia, *aph*(3')-IIIa, *aph*(2'')-Ih) were prevalent in our collection, detection of the *msrA* and *mphC* genes increased significantly in pandemic *S. aureus* isolates. Similarly, we observed a higher prevalence of isolates carrying the genes encoding the Clumping Factors A and B, involved in fibrinogen binding. Of note, macrolides were extensively used as accessory therapy for COVID-19 and fibrinogen levels were usually elevated upon SARS-CoV-2 infection. Therefore, our results reveal a remarkable adaptation of the *S. aureus* isolates to the COVID-19 pandemic context and demonstrates the potential of whole-genome sequencing to conduct molecular epidemiology studies.

2

54 **INTRODUCTION**

55 Bacteremia is a life-threatening condition with high morbidity and mortality rates that can elicit

56 a systemic host response known as sepsis (Viscoli 2016). These episodes often result in

57 complicated bacteremia, usually defined by the presence of attributable mortality, the

58 development of hematogenous embolisms (i.e. endocarditis, discitis, osteomyelitis of systemic

59 abscesses) or the persistence of viable bacteria in blood after three or more days after proper

60 antibiotic treatment (Gudiol et al. 2015). *Staphylococcus aureus* is among the top species causing

61 bacteremia-associated mortality (Kern and Rieg 2020) and persistent bacteremia (Wiggers et al.

62 2016), which in turn is linked to a higher risk of metastatic spread (Khatib et al. 2006). There is

63 increasing awareness that patients who survive sepsis often have long-term physical,

64 psychological and cognitive disabilities with significant health care and social implications

65 (Singer et al. 2016).

66 Several host factors such as certain comorbidities, the setting of the infection onset and the

67 severity of sepsis, have been associated with the high mortality rates observed in *S. aureus*

68 bacteremia (van Hal et al. 2012; Yilmaz et al. 2016). However, the patient's age is the most

69 consistent predictor of mortality, with older patients being twice as likely to die (van Hal et al.

70 2012). Also, certain strain characteristics such as methicillin resistance have also been shown to

71 impact the clinical outcome (Lee et al. 2018). In contrast, the role of specific genetic traits of *S.*

72 *aureus* in the evolution of bacteremia is much less understood. Recent studies suggest that *S.*

73 *aureus* genetic factors predictive of infection evolution may be lineage specific, which would

74 hinder their identification (Gasch et al. 2013; Recker et al. 2017).

75 *S. aureus* has also been described as a leading cause of secondary infection during past viral

76 pandemics, significantly increasing patient mortality rates (Chertow and Memoli 2013). In this

77 regard, recent reports have noted a higher incidence of bacteremia by *S. aureus* at the beginning

78 of the COVID-19 pandemic (Falces-Romero et al. 2023). In the same line, our group has recently

79 reported a rise of vascular catheter-related bacteremia in early 2020. Moreover, we also

80 observed a significant increase in cases of *S. aureus* bacteremia (Gasch et al. 2022). However,

81 while several studies have addressed the incidence, prevalence and clinical outcomes of SARS-

82 CoV-2 and *S. aureus* co-infection (Adler et al. 2020; Adalbert et al. 2021), the genomic

83 differences between such strains and those isolated in the pre-pandemic times have not been

84 explored.

85 Here, we investigated the clinical aspects, epidemiology and genomic features of 339 *S. aureus*

86 strains isolated from patients with bacteremia at the Parc Taulí University Hospital before and

87   during the COVID-19 pandemic (2014-2022). This analysis allowed us to shed light into significant

88   associations between *S. aureus* lineages, antibiotic resistance genes, virulence factors and the

89   clinical outcome of bacteremia. Comparative genomics analysis pointed out that some virulence

90   factors and antibiotic resistance genes were enriched in pandemic *S. aureus* isolates.

91

92   **MATERIAL AND METHODS**

93   **Cohort and strain isolation**

94   **Patients and setting.** All consecutive adult patients (≥18 years) diagnosed with *S. aureus*

95   bloodstream infection from July 2014 to December 2022 at the Parc Taulí University Hospital

96   (Sabadell, Spain) were retrospectively included in this study.

97   **Clinical data.** Clinical information was recorded including patient demographics, comorbidities

98   and other clinical characteristics, source of bacteremia, place of acquisition, severity of sepsis,

99   antibiotic therapy and infection outcomes. The modified Charlson score (Charlson et al. 1987)

100   was used to assess patient morbidities. Setting of acquisition was classified according to

101   modified Friedman criteria (Friedman et al. 2002) as: community, in-hospital acquired or

102   healthcare-related. 30-day mortality was considered as any death within the first month after

103   the bloodstream infection onset. Persistent bacteremia was defined as the presence of positive

104   blood cultures after 72 hours of appropriate antibiotic therapy. Septic embolism was

105   determined as the presence of one or more diagnosed secondary foci as a result of bacterial

106   spread through blood. Strains isolated from March 14th 2020 (Spain's lockdown start) onwards

107   were considered as pandemic clones. These data are available in Data S1**.**

108   **Strain isolation and manipulation.** For each patient, only the first episode of *S. aureus*

109   bacteremia was included in the analysis. Blood cultures were processed using the BACT/ALERT®

110   automated system (bioMérieux) following standardized procedures. *S. aureus* strains were

111   identified by using mass spectrometry technology (MALDI-TOF MS, Bruker). *S. aureus* single

112   colonies were frozen and stored at -80°C. Antibiotic susceptibility testing was assessed by

113   microdilution methodology according to standardized protocols using the MicroScan WalkAway

114   system® (Beckman Coulter).

115   **Ethics Statement:** The Ethics Committee for Investigation with medicinal products (CEIm) of the

116   Parc Taulí University Hospital approved the implementation of this study (2023/5088, approved

117   on 6 October 2023). The requirement for informed written consent was waived given the

118   retrospective nature of the study. Patient identification was encoded, complying with the

119   requirements of the Spanish Organic Law on Data Protection 15/1999.

4

120

Whole-genome sequencing and *de novo* assembly

DNA extraction. *S. aureus* isolates were grown on Columbia Agar with 5% Sheep Blood plates (bioMérieux) at 37°C. Total DNA was purified using the DNeasy Blood & Tissue Purification Kit (Qiagen) following the manufacturer's instructions. Cell lysis was achieved by pre-incubating bacterial colonies in Phosphate-buffered saline (PBS) containing 100 µg/mL lysostaphin (Merck) at 37ºC for 30 minutes. DNA quality was assessed using a NanoDrop device (Thermo Fisher Scientific) and a Qubit® 2.0 fluorometer (Thermo Fisher Scientific).

DNA sequencing. Libraries for sequencing were prepared with the Nextera XT DNA Sample Preparation Kit (Illumina). Whole-genome sequencing was performed using paired-end sequencing on an Illumina HiSeq 2500 and NovaSeq 600 sequencers available at the Genomics Unit of the Centre de Regulació Genòmica (CRG, Barcelona). Whole-genome sequencing data are available at National Center for Biotechnology Information (NCBI) under the accession number PRJNA1055690.

Quality control. The quality of the raw sequencing reads was checked with FastQC (Andrews 2010). Read pre-processing and filtering were performed with TrimGalore (Krueger 2012) by shaving the sequencing adapters, trimming the initial 20 bp poor-quality positions and using a Phred score >= 20 limit.

***De novo* assembly.** The trimmed paired-end reads were assembled *de novo* using shovill (Seemann 2023) and annotated with prokka (Seemann 2014) against the COG (Galperin et al. 2021), HAMAP (Pedruzzi et al. 2015) and Pfam (Mistry et al. 2021) databases and using the *S. aureus* NCTC 8325 [NC_007795] proteome as the reference. CheckM2 was finally used for assessing the quality of assemblies (Chklovski et al. 2023).

143

Isolate typing and *S. aureus* annotation

Isolate typing. Multilocus sequence typing (MLST) was carried out on the assembled scaffolds using the MLST software (Larsen et al. 2012). Sequence Types (ST) and Clonal Complexes (CC) were deduced from the *S. aureus* PubMLST database (Jolley et al. 2018) grouping the *arcC, aroE, glpF, gmk, pta, tpi* and *yqiL* gene types. spaTyper was used to assign *spa* types according to the Ridom Spa Server database guidelines (Sanchez-Herrero 2020), AgrVATE was used for *agr* typing (Raghuram et al. 2022) and SCCmec-types were obtained using SCCmecFinder (Kaya et al. 2018).

Antibiotic resistance genes and virulence factors. Putative antibiotic resistance genes (ARG) and virulence factors (VF) were predicted on the assembled scaffolds with ABRicate (Seemann

5

153   2017) using the in-built NCBI AMRFinderPlus database (Feldgarden et al. 2019) and Virulence

154   Factor Database (VFDB) (Liu et al. 2019), respectively. Strains were considered as Panton-

155   Valentine leukocidin (PVL) positive when both *lukF* and *lukS* genes were predicted on the same

156   genome.

157   **Plasmid prediction.** Plasmid scaffolds were identified using MOB-recon and mobility was

158   predicted based on the MOB-typer module (Robertson and Nash 2018). PlasmidFinder software

159   from Center for Genomic Epidemiology (CGE) was used for *rep* typing (Carattoli et al. 2014) and

160   roary for identifying plasmid core genes (Page et al. 2015).

161   **Prophage prediction.** Prophage prediction was performed as described recently for other *S.*

162   *aureus* genomes (Sweet et al. 2023). Prophage regions were detected in assembled scaffolds

163   using PhiSpy (Akhter et al. 2012) and CheckV was then used to remove host contamination and

164   to delimit phage boundaries (Nayfach et al. 2021). Prophage clustering was carried out with

165   usearch (Edgar 2010) so that sequences showing 90% similarity along their 90% length were

166   counted as the same. Integrase detection and typing was assessed with BLASTP (Altschul et al.

167   1990) using previously reported integrase sequences (Goerke et al. 2009) as queries and limiting

168   the e-value to $1e^{-20}$ and query coverage to >75%. Each putative integrase identified in the

169   prophage regions was classified into an integrase group according to the query with the lowest

170   e-value in the BLASTP analysis.

171   **Statistical methods**

172   Mann-Whitney U (MWU) test was used for continuous variables and Fisher's exact test (FT) for

173   categorical variables. For clonal associations, MWU was first applied to determine biased

174   distributions of lineages when analyzing a specific genetic feature. If the lineage distributions

175   differed significantly when compared to global frequencies, FT was independently applied to

176   determine the association of each feature with specific lineages. Clonal associations were only

177   computed for strains with known lineage. Always a *p*-value threshold of 0.05 was considered as

178   significant. Statistical analyses were performed using custom Python scripts.

179

180

181   **RESULTS**

182   **Cohort description.** We identified 339 consecutive adult patients diagnosed with *S. aureus*

183   bloodstream infections between 2014 and 2022 (Data S1). Most of them were male (69.3%) and

184   the mean age was 63.7 ± 19.9 years. The calculated Modified Charlson Score was greater or

185   equal than 4 in 64.0%. The most frequent clinical conditions detected were diabetes (31.6%),

6

186   the presence of a foreign device (25.4%), ischemic heart disease (17.7%), congestive heart

187   failure (16.5%), solid neoplasm (15.3%), peripheral arteriopathy (12.7%) and chronic obstructive

188   pulmonary disease (10.0%). Acquisition was nosocomial in 56.6%, while 27.4% were community-

189   acquired and 16.0% healthcare related. Regarding the primary source of infection, vascular

190   catheters (31.8%) and skin infections (18.0%) were predominant, followed by pneumonia (9.4%).

191   As far as 30.7% episodes were of unknown origin (n=104). Antibiotic susceptibility tests indicated

192   that 13.9% infections were caused by methicillin-resistant *S. aureus* (MRSA) strains (Data S1).

193   Regarding clinical outcomes, 93 cases were fatal (27.4%) and the median time to patient's death

194   was 20 (interquartile 25 (IQ25)=8, interquartile 75 (IQ75)=37) days (Data S1). Fatal bacteremia

195   episodes showed to be significantly associated with age, modified Charlson, sepsis, congestive

196   heart failure, immunosuppressive chemotherapy treatment, endocarditis and the presence of a

197   cardiac device (Table S1). Of note, catheter-related bacteremia episodes were less lethal ($p <$

198   0.05) (Table S1). On the other hand, persistent bacteremia was observed in 19.5% of episodes,

199   with the median duration being 43 (IQ25=24, IQ75=67.5) days (Data S1). Persistent infections

200   were significantly associated with sepsis (Table S1). Pneumonia-originated bacteremia never

201   resulted in persistent infections or septic emboli infections ($p < 0.05$) (Table S1). Septic emboli

202   were diagnosed in 24.2% (Data S1) which were more prevalent in community-acquired

203   infections ($p < 0.05$) (Table S1). Septic emboli infections were significantly associated with

204   infective endocarditis episodes (Table S1).

205   **Isolate typing.** The MLST software classified our *S. aureus* isolates in 24 different lineages (Figure

206   1A, Data S1). The major identified lineages were CC30 (19.5%), CC5 (17.1%), CC45 (12.1%), ST398

207   (8.8%), CC8 (8.8%), CC22 (8.0%) and CC15 (5.9%). 18 isolates could not be classified into a known

208   sequence type. The distribution of lineages remained relatively stable over the years of study

209   (Figure 1B).

210   We found significant associations between specific lineages and clinical data. CC5 and CC8

211   strains were more frequently recovered from patients with pneumonia-related bacteremia,

212   while CC30 isolates were more prevalent among bacteremia from surgical site infections ($p <$

213   0.05) (Figure S1, Table S2). Although we did not find any significant association, CC1 and CC8

214   infections showed the highest mortality rates (45.4% and 40.0%, respectively). CC15, CC30,

215   CC45, CC21 and ST398 lineages generated persistent infection with frequencies ranging from

216   20.0 to 25.0%, while CC1 (9.1%) and CC22 (7.4%) were the lineages generating fewer persistent

217   infections. The strains most frequently associated with septic emboli were CC15 and CC45

218   (30.0% and 34.1%) while those that formed the least were CC1 and CC8 (9.1% and 10.0%) (Data

219   S1).

220   MRSA strains belonged more frequently to CC5 (42.5%) and CC8 (38.3%) lineages ($p < 0.05$)

221   (Figure S1, Table S2) but methicillin resistance was also found in CC22 (8.5%), CC45 (4.2%) strains

222   and unknown lineages (6.5%) (Data S1). The vast majority (95.7%) of SCCmec cassettes were

223   grouped into type IV, except for two SCCmec cassettes classified as type V (Data S1). SCCmec

224   type IVc was associated with CC5 and CC8 while SCCmec type IV was linked to CC5 and CC22

225   clones ($p < 0.05$) (Figure S1, Table S2). In our collection, we did not find any association of MRSA

226   strains with mortality (Matthews Correlation Coefficient (MCC) = 0.06).

227   Our analysis predicted that 13 isolates from our collection were *agr*-negative. Among the *agr*-

228   positive strains, 48.5% were classified as type I, 26.1% type II, 22.1% type III and 3.3% type IV

229   (Data S1). We observed a biased distribution of lineages regarding the *agr* types II and III ($p <$

230   0.05) (Figure S1). Specifically, we found that type II *agr* was associated with CC5 and CC15

231   isolates, while type III was almost exclusive of CC30 clones ($p < 0.05$) (Table S2). Finally, our

232   typing analysis revealed 123 different *spa* types (Data S1), being t012 significantly associated

233   with CC30 isolates, t002 and t067 with CC5, t008 with CC8, t084 with CC15 and t1451 with ST398

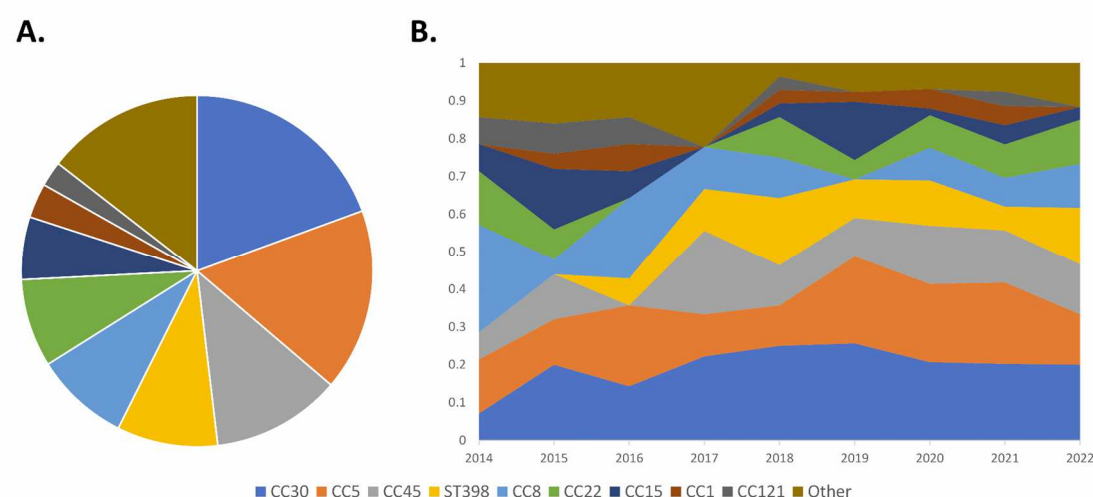234   (Figure S1, Table S2).

235

236   **Figure 1.** (A) Pie chart depicting global *S. aureus* lineage frequencies in our collection. (B)

237   Graphical representation of *S. aureus* lineage frequencies over years. Lineages with less than 5

238   representatives are collected under the umbrella term "Other".

239   **Antibiotic resistance genes.** We identified homologs to 34 different ARG families conferring

240   resistance to clinically relevant antibiotics (Figure 2, Data S1). Homologs of the *mecA* gene were

8

241   found in 47 strains (13.9%) and they were associated primarily with CC5 and CC8 strains ($p <$

242   0.05) (Figure S1, Table S2).

243   Homologs of genes related to tetracycline, β-lactams and fosfomycin resistance were the most

244   prevalent. Homologs of *tet38* were identified in all isolates, of complete *blaI-blaR-blaZ* clusters

245   in 279 strains (82.3%) and of *fosB* in 206 (60.2%). We found that the *blaZ$_{PC1}$* variant was mainly

246   associated with strains belonging to the CC30 lineage ($p < 0.05$) (Figure S1, Table S2). All isolates

247   belonging to CC5, CC8, CC15, CC30 and CC121 lineages encoded a *fosB* gene homolog. In

248   contrast, CC22, CC45 and ST398 clones did not present any fosfomycin resistance gene

249   homologs (Table S2).

250   In addition, we identified homologs to three different groups of genes conferring macrolide

251   resistance: several *erm* variants encoding 23S rRNA methylases (19.5%), the ABC-F type

252   ribosomal protection encoding gene *msrA* (10.0%) and the phosphotransferase gene *mphC*

253   (9.4%). We observed a strong correlation between homologs of *mphC* and *msrA* (MCC = 0.97),

254   which were significatively associated with CC5 and CC8 lineages (Figure S1, Table S2). In addition,

255   almost all strains carrying *ermT* belonged to the ST398 sequence type ($p < 0.05$) (Figure S1, Table

256   S2). Homologs of *ermA* were associated with CC1 and CC5 while *ermC* homologs were linked to

257   CC8 clones ($p < 0.05$) (Figure S1, Table S2). We also detected a biased distribution of the

258   aminoglycoside nucleotidyltransferase genes *ant*(4')-Ia (9.1%) and *ant*(9)-Ia (5.9%) as well as of

259   the aminoglycoside phosphotransferase genes *aph*(3')-IIIa (7.4%) and *aph*(2'')-Ih (4.4%) (Figure

260   S1). Specifically, *ant*(4')-Ia gene homologs were significatively associated with CC5 and CC8

261   strains, *ant(9)*-Ia with CC1 and CC5, *aph(3')*-IIIa with CC5 and CC8, and *aph(2'')*-Ih with ST398

262   (Table S2). Homologs of the bleomycin resistance gene *bleO* (7.4%) showed a positive correlation

263   with *ant*(4')-Ia (MCC = 0.89) and were also linked to CC5 and CC8 clones ($p < 0.05$) (Figure S1,

264   Table S2). Finally, homologs of the *mupA* gene (3.8%), conferring mupirocin resistance, were

265   significatively associated with CC30 isolates (Figure S1, Table S2).
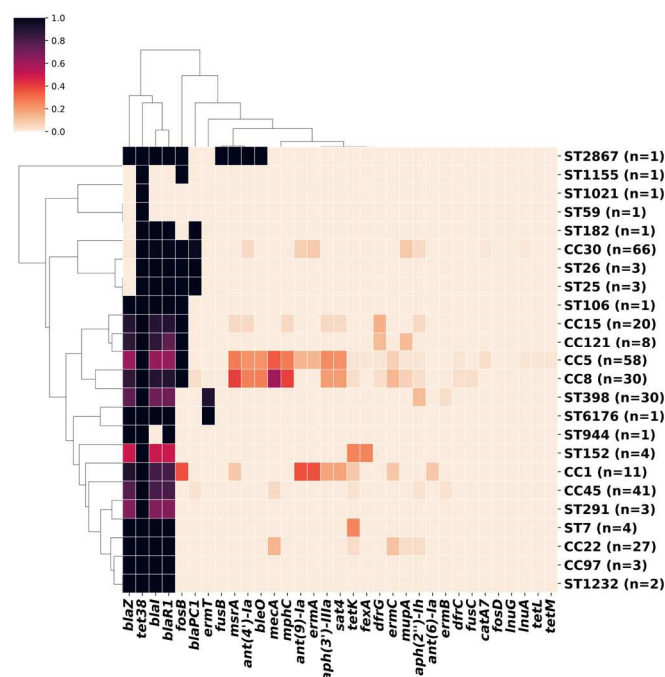
266

Figure 2. Clustered heatmap representing the frequency of abricate-predicted ARGs for all *S. aureus* lineages. Cells are colored from pale orange (0%) to black (100%). Samples were clustered and visualized using the Seaborn clustermap function. Isolates with unknown lineage were not included.

Virulence factors. The presence of VF contributing to *S. aureus* pathogenicity and invasiveness was predicted (Figure 3, Data S1). All isolates from our collection carried homologs of the *cap* gene cluster responsible for the synthesis of capsular polysaccharide. Capsular polysaccharide serotype 8 was significatively more prevalent in CC15, CC30, CC45 and CC121 lineages (Figure S1, Table S3) while serotype 5 were mainly found at CC5, CC8, CC22 and ST398 clones. Homologs of the Immune Evasion Cluster (IEC) (*sak*, *chp* and *scn*) and *sbi*, also involved in immune system evasion, were present in 73.1 - 99.4% of the isolates. The *sak* gene was not found in ST398 isolates. Similarly, 99.7% of the isolates carried the *isdA-G* gene homologs, which confer resistance to killing by human lactoferrin. The intracellular adhesion (*ica*) locus, involved in cell-cell adherence and biofilm formation, was detected in all strains. Homologs of genes coding for several Microbial Surface Components Recognizing Adhesive Matrix Molecules (MSCRAMMs) were also detected, although to different extents: *ebp* (95.3%), *eap/map* (93.5%), *sdrC* (92.0%), *sdrE* (87.6%), *clfA* (86.1%), *fnbA* (74.6%), *clfB* (68.4%), *fnbB* (62.2%), *sdrD* (53.7%), *vWbp* (47.8%) and *cna* (15.9%). Specifically, we found that the secreted von Willebrand factor-binding protein (*vWbp*) was more prevalent in CC1, CC8, CC30, CC45 and CC121 lineages while the *cna* gene was associated with CC30 clones ($p < 0.05$) (Figure S1, Table S2).

10

287   Almost all isolates carried homologs of the genes encoding the α-, β- and δ- hemolysins (*hla*, *hlb*,

288   *hlgABC* and *hld*). Genes responsible for the formation of type VII secretion systems (T7SS), *esa*,

289   *ess* and *esx*, were also widespread in our collection. Enterotoxin-encoding genes (*sea, seb, sec,*

290   *sed, seh, selk, sell* and *selq*) showed markedly different frequencies ranging from 31.0% (*sea*) to

291   2.9% (*selk* and *selq*) and significatively biased distributions among different lineages (Figure S1).

292   Specifically, CC1 strains were associated with *seb*, *seh*, *selk* and *selq*; CC5 with *sea* and *sed*; CC8

293   with *sea*, *selk* and *selq*; CC30 with *sea* and *seh*; CC45 with *sea*, *sec* and *sell*; and CC121 with *seb*

294   ($p < 0.05$) (Table S2). Of note, *sec* and *sell* genes were totally correlated (MCC = 1.0). We also

295   detected the presence of the toxic shock syndrome toxin-1 (*tsst*-1) gene homologs in 56 isolates

296   (16.5%), which were linked to CC22 and CC30 ($p < 0.05$) (Figure S1, Table S2). In addition, 11

297   isolates were predicted to encode the PVL genes (*luk*F and *luk*S) with a linkage to CC8 strains

298   (Figure S1, Table S2). Finally, we also found homologs of the toxin-encoding genes *eta* (2.1%)

299   and *etb* (0.9%) in our strains.

300

302   **Figure 3.** Clustered heatmap representing the frequency of abricate-predicted VFs for all *S.*

303   *aureus* lineages. Cells are colored from pale orange (0%) to black (100%). Samples were clustered

304   and visualized using the Seaborn clustermap function. Isolates with unknown lineage were not

305   included.

306   **Plasmids.** We identified 51 different plasmids distributed in 256 isolates (75.5%) (Figure 4, Data

307   S1). Among them, the vast majority (52.8%) presented a single plasmid, but we also found strains

308   with two (18.3%), three (3.2%) or four (1.2%) plasmids.

11

309   The core proteome of the most prevalent plasmid, AA410 (n=72; *rep5a/rep16/rep19*), showed

310   heavy metal resistance (*arsB, arsC, cadA, cadC, copB* and *mco*) and lactococcin synthesis genes

311   (Table S3). This plasmid was linked to CC30 strains ($p < 0.05$) (Figure S1, Table S2). Plasmid AA411

312   (n=56; *rep5a/rep16*), harbored the *blaI-blaR-blaZ* cluster for penicillin resistance, a cadmium

313   resistance cluster (*cadC, cadD*) and lactococcin-synthesis genes (Table S3). In this case, AA411

314   plasmids were significantly associated with CC1, CC15 and CC45 (Figure S1, Table S2). Plasmid

315   AA840 (n=33; *rep16/rep19/rep21*), encoding *cadA* gene for cadmium resistance and several

316   ARGs (*blaI-blaR-blaZ, aph(3')-IIIa, mphC, msrA* and *sat4*) (Table S3), was more prevalent among

317   CC5 and CC8 isolates ($p < 0.05$) (Figure S1, Table S2) and showed a positive correlation with

318   MRSA strains (MCC = 0.73). Also significatively associated with these lineages (Figure S1, Table

319   S2) was the AA851 plasmid (n=22, *rep22*) which harbored cadmium resistance genes (*cadC*,

320   *cadD*), the *blaI-blaR-blaZ* cluster and genes for lactococcin synthesis (Table S3). On the other

321   hand, the plasmid AB641 (n=25; *rep13*), which was almost exclusively detected in isolates from

322   the ST398 lineage ($p < 0.05$) (Figure S1, Table S2), carried two cadmium resistance genes (*cadC*,

323   *cadD*) and the macrolide-resistance gene *ermT* (Table S3)*.* Finally, plasmid AC670 (n=19;

324   *rep7c/rep16/rep19/rep22*) encoded genes conferring antimicrobial resistance (*ant(4')-Ia, bleO*);

325   and plasmid AA848 (n=15; *rep20*) carried several ARGs (*blaI-blaR-blaZ, mphC, msrA* and *tetK*),

326   two cadmium resistance loci (*cadC*, *cadD*) and the staphylococcal enterotoxin D-encoding (*sed*)

327   gene (Table S3). AC670 plasmids were associated with CC5 and CC8 clones while AA848 plasmids

328   were linked to CC5 clones ($p < 0.05$) (Figure S1, Table S2).

329   We also predicted other less-abundant plasmids, carrying other genes conferring resistance to

330   aminoglycosides (*ant(6)-Ia, aph(2'')-Ih*), macrolides (*ermA, ermB, ermC, msrA, mphA*),

331   tetracycline (*tetK*), chloramphenicol (*catA7*), lincosamides (*lnuA*) and trimethoprim (*dfrG*). The

332   exfoliative toxin B encoding gene (*etb*) was also annotated in three plasmids (Table S3).

333   Overall, our results showed that *ant(6)-Ia, aph(3')-IIIa, catA7, ermC, lnuA, mphC, msrA* and *sat4*

334   genes were exclusively plasmid-borne in our collection (Figure S2). Likewise, *mupA* (92.3%),

335   *ant(4')-Ia* (90.3%), *bleO* (88.0%), *ermT* (80.6%) and *tetK* (77.8%) genes were also much more

336   prevalent in plasmids than in chromosomes. Similarly, around 50% of the *blaI-blaR-blaZ* cluster

337   was detected in plasmids. In contrast, several abundant genes such as *ant(9)-Ia, ermA, fosB,*

338   *mecA* or *tet38* were always chromosomally encoded (Figure S2). Finally, the virulence genes *sed*

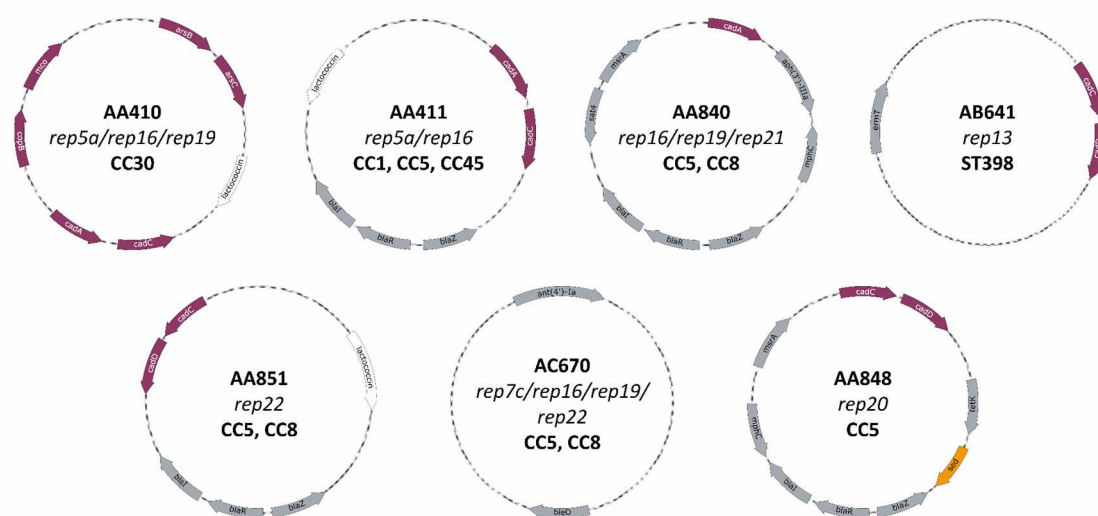339   and *etb* were found to be exclusively plasmid-borne.

340

Figure 4. Schematic representation of the most abundant plasmids in our collection. Gene coloring depicts ARGs (gray), VF (orange), heavy metal resistance genes (purple) and lactococcin synthesis genes (white). Rep types and lineage associations are also included. Only plasmids harbored in more than 15 isolates were included.

Prophages. We predicted 369 different prophage clusters in 336 isolates (97.6%) (Data S1). The majority presented one (28.6%) or two (28.9%) prophages, but we also found strains with three (21.5%), four (12.1%), five (7.4%), six (0.9%) or even seven (0.6%) prophage sequences.

Prophage clusters from the integrase group 3 (Sa3) were predominant in our collection (n=43). Some of them (n=15) carried homologs of complete IEC (*scn*, *chp*, *sak*). Enterotoxin A encoding gene (*sea*) was predicted in six of them and *tsst-1* was found in one cluster (Table S4). Of note, different Sa3-prophage clusters (1, 15, 29 and 55) showed a biased distribution in our collection (Figure S1). Specifically, cluster 1 was associated with CC30, cluster 15 with ST398, cluster 29 with CC5 and, finally, cluster 55 with CC30 and ST398 strains ($p < 0.05$) (Table S2).

We further identified some prophage clusters (n=26) of the integrase group 2 (Sa2), two of them encoding *sea* and *tsst-1* genes. We also predicted 24 prophage clusters from integrase group 1 (Sa1); 22 from integrase group 5 (Sa5), with two harboring *sec* and *sell* genes; and 17 from integrase group 6 (Sa6). Prophages from integrase group 7 (Sa7) and 9 (Sa9) were also identified but to a lesser extent. Finally, 221 prophage clusters did not present any integrase gene. Among those, 14 clusters carried a complete IEC and 10 harbored the *sea* gene (Table S4).

No ARG were detected in the predicted prophage genomes.

13

361   **Pandemic-associated features.** We identified 139 and 200 consecutive adult patients diagnosed

362   with bloodstream infections by *S. aureus* before and after March 14th 2020, respectively (Data

363   S1). In the pre-pandemic years, we detected 27.8 episodes of *S. aureus* bacteremia per year in

364   our hospital rising to 66.7 during the pandemic. In such years, we observed an increase of

365   nosocomial infections, from 69 episodes in the pre-pandemic years to 119 during the COVID-19

366   pandemic. Specifically, cases of *S. aureus* peripheral catheter-related bacteremia were

367   significantly more prevalent and we also found 2.5 times more episodes of bacteremia

368   originating from surgical sites (Table S5). We also identified a significant increase of MRSA

369   infections (p < 0.05) and we diagnosed 2.8 times more endocarditis cases (Table S5).

370   Statistical analysis on pre- and pandemic strains revealed significant genetic differences

371   between these two *S. aureus* populations. We observed a strong increase of strains carrying

372   genes encoding the clumping factors A (*clfA*, p = $2.1e^{-03}$) and B (*clfB*, p = $2.3e^{-05}$) (Table S5).

373   Clumping factors A and B are MSCRAMMs that bind fibrinogen, which is found at high levels

374   upon SARS-CoV-2 infection (O'Brien et al. 2002; Kangro et al. 2022). In contrast, we found a

375   significant reduction of strains encoding the *sdrE* gene, which is also classified as MSCRAMM

376   (Table S5). On the other hand, we noticed a rise in several antibiotic resistance genes during

377   those years. Specifically, the macrolide-resistance *msrA* and *mphC* genes as well as the

378   methicillin-resistance *mecA gene* showed a significant increase during the pandemic years

379   (Table S5). Of note, macrolides were extensively used as accessory therapy for COVID-19 in

380   patients (Sterenczak et al. 2020; Grau et al. 2021).

381

382   **DISCUSSION**

383   **Global insights into *S. aureus* clinics, antibiotic resistance and virulence**

384   Genomics enables unraveling the genetic makeup of pathogens, providing insights into virulence

385   factors, antibiotic resistance mechanisms and the overall pathogenic potential of bacteria. This

386   information is crucial for the development of targeted diagnostics, treatment strategies and

387   preventive measures. The use of genomics also allows tracking the spread of specific strains and

388   identifying emerging threats, contributing to the surveillance and control of infections. Here,

389   using a collection of 339 *S. aureus* isolates from patients with bacteremia, we unveiled important

390   insights into the clinical and genomic features of these bacterial pathogens (Table 1).

391   In our hospital, we identified *S. aureus* lineages mirroring those previously reported in Spain

392   (Pérez-Montarelo et al. 2018) and in other countries (Fowler et al. 2007; Park et al. 2017;

393   Campbell et al. 2022) (Figure 1), suggesting a shared genetic heritage and potentially common

394 evolutionary pathways. Pérez-Montarelo and colleagues analyzed strains isolated across various

395 Spanish hospitals spanning 2002 to 2017 (Pérez-Montarelo et al. 2018). Our study, conducted

396 between 2014 and 2022, complements this report and broadens its scope into the pandemic

397 period, offering compelling observations on the evolutionary trends of *S. aureus* clones.

398 Specifically, we observed an increase of ST398 lineages, heightening from 2.4% (Pérez-

399 Montarelo et al. 2018) to a mean prevalence of 8.8% in our isolates. Importantly, the prevalence

400 of this lineage in our collection ranged from 0% (2014 and 2015) to 15% (2022). These results

401 highlight the spread of ST398 lineage in hospital settings, confirming the need to focus on the

402 mechanisms involved in the epidemiological success of ST398 in humans, as previously

403 suggested (Uhlemann et al. 2017; Mama et al. 2021; van der Mee-Marquet et al. 2022) (Figure

404 1).

405 Despite possible associations between genotypes and certain complications, the role of *S.*

406 *aureus* genetic factors in the evolution of bacteremia is still poorly understood. CC1, CC5, CC8,

407 CC22 and CC30 lineages have been associated with increased risk of complications (Fowler et al.

408 2007; Miller et al. 2012). In contrast, more recent studies did not find any apparent association

409 between clonality and poorer outcomes (Chong et al. 2013; Gasch et al. 2014; Fernández-

410 Hidalgo et al. 2018). Our study is in line with the latter since we did not find significant

411 associations between the different isolates from our collection and clinical outcome. However,

412 there is a tendency for the CC1 and CC8 strains to cause fatal infections. On the other hand, we

413 identified associations between the different lineages and the focus of infection. CC5 and CC8

414 were correlated with pneumonia-originated bacteriemia, as deduced from previous reports

415 (Antonelli et al. 2019), and CC30 with surgical site infections (Table 1, Table S2).

416 MRSA poses a significant public health concern due to its ability to cause infections that are

417 challenging to treat, showing higher mortality than MSSA infections (Munckhof et al. 2008). In

418 Spain, the prevalence of methicillin resistance among *S. aureus* isolates is around 20-25% (Pérez-

419 Montarelo et al. 2018; Vázquez-Sánchez et al. 2022), while the incidence of MRSA infections in

420 our hospital showed to be 13.9% (Figure 2). Of note, we did not find associations with mortality

421 and MRSA strains. In accordance with some reports, most of our MRSA isolates belonged to CC5

422 or CC8 strains (Dupper et al. 2019). These lineages were also the ones accumulating more

423 antibiotic resistance genes (Figure 2, Table 1), as previously stated (Smith et al. 2021). Genes

424 predicted to confer resistance to tetracycline and β-lactams were the most prevalent in our

425 isolates (Figure 2). However, the results for tetracycline did not align well with the patterns

426 observed *in vitro* by broth microdilution tests. The *tet38* gene, which was present in almost all

16bioRxiv preprint doi: https://doi.org/10.1101/2023.12.22.572975; this version posted December 22, 2023. The copyright holder for this preprint (which was not certified by peer review) is the author/funder, who has granted bioRxiv a license to display the preprint in perpetuity. It is made available under a CC-BY-NC-ND 4.0 International license.

427 strains, is known to confer tetracycline resistance when overexpressed (Chen and Hooper 2018),

428 but its mere presence does not necessarily indicate resistance to this class of antibiotics.

429 *S. aureus* is known for its pathogenic potential, primarily attributed to a diverse set of virulence

430 factors. As previously elucidated, the *agr* groups and capsular polysaccharide serotypes were

431 associated with *S. aureus* clonality (Figure 3, Table 1) (Monecke et al. 2011). Several genes

432 involved in immune system evasion (*adsA*, *aur*, *sbi, ssl, sspA, sspB*), lactoferrin resistance (*isdA-*

433 *G*), adhesion (*ica*), T7SS formation (*esa, ess, esx*), some MSCRAMMs (*ebp*, *eap/map*, *sdrC*) and

434 hemolysins were found in virtually all strains (Figure 3), similar to previous reports (Rasmussen

435 et al. 2013). IEC is an immune response cluster harboring *chp*, *scn* and *sak* genes which is typically

436 encoded by β-hemolysin converting bacteriophages (Sieber et al. 2020). This is partially

437 paralleled in our isolates, in which we predicted 61.7% of complete IEC clusters in prophage

438 regions (Table S4). In contrast to many other bacterial pathogens, *S. aureus* produces a wide

439 array of toxins (Cheung et al. 2021). In our hospital, besides hemolysins, the most abundant

440 predicted toxins were the exotoxins SEA (31.0%) and TSST-1 (16.5%), the latter being the major

441 cause of toxic shock syndrome (Figure 3). SEA is the most common staphylococcal enterotoxin

442 (Pinchuk et al. 2010) and is also reported to be encoded by a prophage (Betley and Mekalanos

443 1985). In our isolates, only 53.8% of *sea* genes were predicted in prophage regions (Table S4),

444 hereby indicating that we could be underestimating prophage regions. Finally, we found 11 PVL-

445 positive strains (3.2%) (Figure 3). Panton–Valentine leukocidin is a pore-forming leukotoxin

446 produced by 2-3% of *S. aureus* isolates (Wójcik-Bojek et al. 2022) which has been traditionally

447 used as an indicator of community-acquired MRSA strains (Fey et al. 2003). However, some

448 recent studies found that PVL may not be a reliable marker because it is being reported in

449 nosocomial MRSA infections (Nakaminami et al. 2020; Shohayeb et al. 2023). Paralleling these

450 reports, we found 4 non-community MRSA harboring PVL suggesting a possible spread of these

451 strains in hospitals.

452

453

454

455

456

457

458   **Table 1.** Summary of the significant associations between the most abundant *S. aureus* lineages

459   with all the clinical and genetic data.

Lineage	Clinical features	Gene types	Antibiotic Resistance Genes	Virulence Factors	Plasmids	Prophages
CC1			*ant*(9)-Ia, *ermA*	*seb, seh, selk, selq*	AA411	
CC5	MRSA, pneumonia-originated bacteremia	SCCmec IVc, *agr* type II, *spa* t002, *spa* t067	*ant(4')*-Ia, *ant*(9)-Ia, *aph(3')*-IIIa, *bleO, ermA, fosB, mecA, mphC, msrA*	*cap5, sea, sed*	AA840, AA851, AC670, AA848	cluster_29 (Sa3)
CC8	MRSA, pneumonia-originated bacteremia	SCCmec IVc, *spa* t008	*ant(4')*-Ia, *aph(3')*-IIIa, *bleO, ermC, fosB, mecA, mphC, msrA*	*cap5, sea, selk, selq*, PVL	AA840, AA851, AC670	
CC15		*agr* type II, *spa* t084	*fosB*	*cap8*	AA411	
CC22		SCCmec IV		*cap5, tsst-1*		
CC30	Bacteriemia from surgical site infections	*agr* type III, *spa* t012,	*blaZPC1, fosB, mupA*	*cap8, sea, seh, tsst-1*	AA410	cluster_1 (Sa3), cluster_55 (Sa3)
CC45				*cap8, sea, sec, sell*	AA411	
CC121			*fosB*	*cap8, seb*		
ST398		*spa* t1451	*aph(2'')*-Ih, *ermT*	*cap5*	AB641	cluster_15 (Sa3), cluster_55 (Sa3)

460

Changes in molecular characteristics of pandemic *S. aureus* isolates

462   Understanding the interplay between viral and bacterial infections, including the prevalence and

463   impact of *S. aureus* in COVID-19 cases, is important for effective patient care and public health

464   measures. Several studies underscored a higher incidence of bacteremia by *S. aureus* at the

465   COVID-19 pandemic (Falces-Romero et al. 2023). In keeping with this, the episodes of *S. aureus*

466   bacteremia per year doubled in our hospital during the pandemic. Concomitantly, we found a

467   rise in nosocomial infections, particularly those originated from catheters and surgical sites. The

468   increase of catheter-related bacteremia during the COVID-19 epidemic has been previously

469   documented by our group (Gasch et al. 2022).

470   Unlike other countries, we did not detect emerging *S. aureus* clones during the pandemic (Gu et

471   al. 2023). However, we noticed a significant increase in strains carrying the *clfA* and *clfB* genes,

472   a reduction of strains encoding *sdrE*, along with a rise in macrolide and methicillin antibiotic

473   resistance genes (Table S5).

17

474   The *clfA* and *clfB* genes are MSCRAMMs encoding the fibrinogen-binding Clumping Factors A

475   and B, respectively. Fibrinogen is one of the most prevalent coagulation proteins in blood

476   (Kangro et al. 2022). ClfA is the major virulence factor responsible for *S. aureus* clumping in blood

477   plasma (O'Brien et al. 2002) and ClfB interacts with cytokeratin 10 and loricrin facilitating *S.*

478   *aureus* skin infection (Lacey et al. 2019). Both ClfA and ClfB have been reported to be involved

479   in bacterial and platelet aggregation (O'Brien et al. 2002). Interestingly, several reports

480   documented an increase of fibrinogen production by SARS-CoV-2 virus (Bouck et al. 2021;

481   Kangro et al. 2022). Therefore, our results suggest that the presence of *clfA* and *clfB* genes

482   provided an advantage to *S. aureus* in the context of SARS-CoV-2 co-infection by enhancing

483   fibrinogen binding. In consequence, *S. aureus* bloodstream isolates carrying the *clfA* and *clfB*

484   genes were positively selected between 2020 and 2022. Conversely, we found a reduced

485   prevalence of the *sdrE* gene, which codes for a MSCRAMM that prevents *S. aureus* phagocytosis

486   by sequestering the human complement factor H (CFH) on the surface of bacterial cells (Zhang

487   et al. 2017; Wójcik-Bojek et al. 2022). This is remarkable because it has been shown that the

488   SARS-CoV-2 spike protein blocks CFH leading to a complement dysregulation on the human cell

489   surface (Yu et al. 2022). Therefore, the functional redundancy of *S. aureus* SdrE and the SARS-

490   CoV-2 spike protein could explain the negative selection of *sdrE*. In the same line, it is important

491   to note that *S. aureus* CflA has also been found to have an anti-phagocytic effect (Higgins et al.

492   2006; Hair et al. 2010).

493   Regarding *S. aureus* antibiotic resistance, some articles have emphasized the role of macrolides

494   as adjunctive therapy for COVID-19 in certain patients (Sterenczak et al. 2020) and the use of

495   such antibiotics could allow selecting resistant strains. Macrolide resistance in staphylococci is

496   mainly associated with mobile ARGs which often correlates with methicillin resistance (Serra et

497   al. 2023), as also observed in our collection (Figure 2). These findings emphasize the evolving

498   nature and impact of *S. aureus* infections in the COVID-19 pandemic era.

499

18

513

514 **CONFLICT OF INTEREST STATEMENT**

515 The authors declare that the research was conducted in the absence of any financial or

516 commercial relationships that could be a potential conflict of interest.

517

518 **DATA AVAILABILITY**

519 Sequence data generated in this study have been deposited in the NCBI database with the

520 following access number: PRJNA1055690. Source data are provided with this paper as

521 Supplementary Material.

522

523 **FIGURES AND TABLES**

524 **Figure 1.** (A) Pie chart depicting global *S. aureus* lineage frequencies in our collection. (B)

525 Graphical representation of *S. aureus* lineage frequencies over years. Lineages with less than 5

526 representatives are collected under the umbrella term "Other".

527 **Figure 2.** Clustered heatmap representing the frequency of abricate-predicted ARGs for all *S.*

528 *aureus* lineages. Cells are colored from pale orange (0%) to black (100%). Samples were clustered

529 and visualized using the Seaborn clustermap function. Isolates with unknown lineage were not

530 included.

531 **Figure 3.** Clustered heatmap representing the frequency of abricate-predicted VFs for all *S.*

532 *aureus* lineages. Cells are colored from pale orange (0%) to black (100%). Samples were clustered

533 and visualized using the Seaborn clustermap function. Isolates with unknown lineage were not

534 included.

535   **Figure 4.** Schematic representation of the most abundant plasmids in our collection. Gene

536   coloring depicts ARGs (gray), VF (orange), heavy metal resistance genes (purple) and lactococcin

537   synthesis genes (white). Rep types and lineage associations are also included. Only plasmids

538   harbored in more than 15 isolates were included.

539   **Table 1.** Summary of the significant associations between the most abundant *S. aureus* lineages

540   with all the clinical and genetic data.

541

542   **SUPPLEMENTARY MATERIAL**

543   **Data S1.** JSON-formatted file including the clinical metadata and predicted features for all *S.*

544   *aureus* strains included in this study.

545   **Figure S1.** Pie plots depicting lineage frequencies for all clinical and genetic features. The MWU

546   *p*-values obtained when comparing to global lineage frequency are included.

547   **Figure S2.** Heatmap representing the frequency of chromosome- or plasmid-encoded genes for

548   all ARGs in *S. aureus* lineages. Cells are colored from blue (all instances are plasmid-borne) to

549   red (all instances are in the chromosome), with white indicating absence of ARG.

550   **Table S1.** Results for statistical analysis of clinical data. In each case, the computed *p*-value and

551   selected statistical method are included.

552   **Table S2.** Results of Fisher's exact test (FT) for analyzing associations between specific *S. aureus*

553   lineages and clinical or genetic data. FT was only computed for features with biased distributions

554   in MWU analysis (Figure S1).

555   **Table S3.** List of predicted plasmids including number of instances, the roary-core proteome,

556   and the abricate-predicted antibiotic resistance genes and virulence factors.

557   **Table S4.** List of predicted prophage clusters including number of instances, integrase type,

558   presence of IEC and the abricate-predicted virulence factors. All phage instances of the same

559   cluster not necessarily harbored all the features.

560   **Table S5.** Results of Fisher's exact test for comparing the clinical and genetic features of pre- and

561   pandemic bacteremia episodes.

562

563   **REFERENCES**

564   Adalbert JR, Varshney K, Tobin R, Pajaro R. 2021. Clinical outcomes in patients co-infected with
565   COVID-19 and *Staphylococcus aureus*: a scoping review. *BMC Infect Dis* **21**: 985.

566   Adler H, Ball R, Fisher M, Mortimer K, Vardhan MS. 2020. Low rate of bacterial co-infection in
567   patients with COVID-19. *Lancet Microbe* **1**: e62.

568   Akhter S, Aziz RK, Edwards RA. 2012. PhiSpy: a novel algorithm for finding prophages in bacterial
569   genomes that combines similarity- and composition-based strategies. *Nucleic Acids Res*
570   **40**: e126.

571   Altschul SF, Gish W, Miller W, Myers EW, Lipman DJ. 1990. Basic local alignment search tool. *J
572   Mol Biol* **215**: 403–410.

573   Andrews S. 2010. FastQC: a quality control tool for high throughput sequence data.
574   https://www.bioinformatics.babraham.ac.uk/projects/fastqc/ (Accessed March 30,
575   2022).

576   Antonelli A, Giani T, Coppi M, Di Pilato V, Arena F, Colavecchio OL, Conte V, Santerre Henriksen
577   A, Rossolini GM, MRSA-HAP Study Group. 2019. *Staphylococcus aureus* from hospital-
578   acquired pneumonia from an Italian nationwide survey: activity of ceftobiprole and
579   other anti-staphylococcal agents, and molecular epidemiology of methicillin-resistant
580   isolates. *J Antimicrob Chemother* **74**: 3453–3461.

581   Betley MJ, Mekalanos JJ. 1985. Staphylococcal enterotoxin A is encoded by phage. *Science* **229**:
582   185–187.

583   Bouck EG, Denorme F, Holle LA, Middelton EA, Blair AM, de Laat B, Schiffman JD, Yost CC,
584   Rondina MT, Wolberg AS, et al. 2021. COVID-19 and Sepsis Are Associated With
585   Different Abnormalities in Plasma Procoagulant and Fibrinolytic Activity. *Arterioscler
586   Thromb Vasc Biol* **41**: 401–414.

587   Campbell AJ, Mowlaboccus S, Coombs GW, Daley DA, Al Yazidi LS, Phuong LK, Leung C, Best EJ,
588   Webb RH, Voss L, et al. 2022. Whole genome sequencing and molecular epidemiology
589   of paediatric *Staphylococcus aureus* bacteraemia. *J Glob Antimicrob Resist* **29**: 197–206.

590   Carattoli A, Zankari E, García-Fernández A, Voldby Larsen M, Lund O, Villa L, Møller Aarestrup F,
591   Hasman H. 2014. In silico detection and typing of plasmids using PlasmidFinder and
592   plasmid multilocus sequence typing. *Antimicrob Agents Chemother* **58**: 3895–3903.

593   Charlson ME, Pompei P, Ales KL, MacKenzie CR. 1987. A new method of classifying prognostic
594   comorbidity in longitudinal studies: development and validation. *J Chronic Dis* **40**: 373–
595   383.

596   Chen C, Hooper DC. 2018. Effect of *Staphylococcus aureus* Tet38 native efflux pump on in vivo
597   response to tetracycline in a murine subcutaneous abscess model. *J Antimicrob
598   Chemother* **73**: 720–723.

599   Chertow DS, Memoli MJ. 2013. Bacterial coinfection in influenza: a grand rounds review. *JAMA*
600   **309**: 275–282.

601   Cheung GYC, Bae JS, Otto M. 2021. Pathogenicity and virulence of *Staphylococcus aureus*.
602   *Virulence* **12**: 547–569.

603 Chklovski A, Parks DH, Woodcroft BJ, Tyson GW. 2023. CheckM2: a rapid, scalable and accurate
604   tool for assessing microbial genome quality using machine learning. *Nat Methods* **20**:
605   1203–1212.

606 Chong YP, Park S-J, Kim HS, Kim ES, Kim M-N, Park K-H, Kim S-H, Lee S-O, Choi S-H, Jeong J-Y, et
607   al. 2013. Persistent *Staphylococcus aureus* bacteremia: a prospective analysis of risk
608   factors, outcomes, and microbiologic and genotypic characteristics of isolates. *Medicine*
609   *(Baltimore)* **92**: 98–108.

610 Dupper AC, Sullivan MJ, Chacko KI, Mishkin A, Ciferri B, Kumaresh A, Berbel Caban A, Oussenko
611   I, Beckford C, Zeitouni NE, et al. 2019. Blurred Molecular Epidemiological Lines Between
612   the Two Dominant Methicillin-Resistant *Staphylococcus aureus* Clones. *Open Forum*
613   *Infect Dis* **6**: ofz302.

614 Edgar RC. 2010. Search and clustering orders of magnitude faster than BLAST. *Bioinformatics* **26**:
615   2460–2461.

616 Falces-Romero I, Bloise I, García-Rodríguez J, Cendejas-Bueno E, SARS-CoV-2 Working Group.
617   2023. *Staphylococcus aureus* bacteremia in patients with SARS-CoV-2 infection. *Med*
618   *Clin (Engl Ed)* **160**: 495–498.

619 Feldgarden M, Brover V, Haft DH, Prasad AB, Slotta DJ, Tolstoy I, Tyson GH, Zhao S, Hsu C-H,
620   McDermott PF, et al. 2019. Validating the AMRFinder Tool and Resistance Gene
621   Database by Using Antimicrobial Resistance Genotype-Phenotype Correlations in a
622   Collection of Isolates. *Antimicrob Agents Chemother* **63**: e00483-19.

623 Fernández-Hidalgo N, Ribera A, Larrosa MN, Viedma E, Origüen J, de Alarcón A, Fariñas MC, Sáez
624   C, Peña C, Múñez E, et al. 2018. Impact of *Staphylococcus aureus* phenotype and
625   genotype on the clinical characteristics and outcome of infective endocarditis.
626   A multicentre, longitudinal, prospective, observational study. *Clin Microbiol Infect* **24**:
627   985–991.

628 Fey PD, Saïd-Salim B, Rupp ME, Hinrichs SH, Boxrud DJ, Davis CC, Kreiswirth BN, Schlievert PM.
629   2003. Comparative molecular analysis of community- or hospital-acquired methicillin-
630   resistant *Staphylococcus aureus*. *Antimicrob Agents Chemother* **47**: 196–203.

631 Fowler VG, Nelson CL, McIntyre LM, Kreiswirth BN, Monk A, Archer GL, Federspiel J, Naidich S,
632   Remortel B, Rude T, et al. 2007. Potential associations between hematogenous
633   complications and bacterial genotype in *Staphylococcus aureus* infection. *J Infect Dis*
634   **196**: 738–747.

635 Friedman ND, Kaye KS, Stout JE, McGarry SA, Trivette SL, Briggs JP, Lamm W, Clark C,
636   MacFarquhar J, Walton AL, et al. 2002. Health care--associated bloodstream infections
637   in adults: a reason to change the accepted definition of community-acquired infections.
638   *Ann Intern Med* **137**: 791–797.

639 Galperin MY, Wolf YI, Makarova KS, Vera Alvarez R, Landsman D, Koonin EV. 2021. COG database
640   update: focus on microbial diversity, model organisms, and widespread pathogens.
641   *Nucleic Acids Res* **49**: D274–D281.

642 Gasch O, Badia-Cebada L, Carmezim J, Vaqué M, Pomar V, Moreno E, Marrón A, Jiménez-
643   Martínez E, García-Quesada MJ, Garcia-Alarcón X, et al. 2022. Effects of the COVID-19

22

644   Pandemic on Incidence and Epidemiology of Catheter-Related Bacteremia, Spain. *Emerg*
645   *Infect Dis* **28**: 2181–2189.

646   Gasch O, Camoez M, Dominguez MA, Padilla B, Pintado V, Almirante B, Martín-Gandul C, López-
647   Medrano F, de Gopegui ER, Ramón Blanco J, et al. 2014. Lack of association between
648   genotypes and haematogenous seeding infections in a large cohort of patients with
649   methicillin-resistant *Staphylococcus aureus* bacteraemia from 21 Spanish hospitals. *Clin*
650   *Microbiol Infect* **20**: 361–367.

651   Gasch O, Camoez M, Dominguez MA, Padilla B, Pintado V, Almirante B, Molina J, Lopez-Medrano
652   F, Ruiz E, Martinez JA, et al. 2013. Predictive factors for mortality in patients with
653   methicillin-resistant *Staphylococcus aureus* bloodstream infection: impact on outcome
654   of host, microorganism and therapy. *Clin Microbiol Infect* **19**: 1049–1057.

655   Goerke C, Pantucek R, Holtfreter S, Schulte B, Zink M, Grumann D, Bröker BM, Doskar J, Wolz C.
656   2009. Diversity of prophages in dominant *Staphylococcus aureus* clonal lineages. *J*
657   *Bacteriol* **191**: 3462–3468.

658   Grau S, Hernández S, Echeverría-Esnal D, Almendral A, Ferrer R, Limón E, Horcajada JP, Catalan
659   Infection Control and Antimicrobial Stewardship Program (VINCat-PROA). 2021.
660   Antimicrobial Consumption among 66 Acute Care Hospitals in Catalonia: Impact of the
661   COVID-19 Pandemic. *Antibiotics (Basel)* **10**: 943.

662   Gu J, Shen S, Xiong M, Zhao J, Tian H, Xiao X, Li Y. 2023. ST7 Becomes One of the Most Common
663   *Staphylococcus aureus* Clones After the COVID-19 Epidemic in the City of Wuhan, China.
664   *Infect Drug Resist* **16**: 843–852.

665   Gudiol F, Aguado JM, Almirante B, Bouza E, Cercenado E, Domínguez MÁ, Gasch O, Lora-Tamayo
666   J, Miró JM, Palomar M, et al. 2015. Executive summary of the diagnosis and treatment
667   of bacteremia and endocarditis due to *Staphylococcus aureus*. A clinical guideline from
668   the Spanish Society of Clinical Microbiology and Infectious Diseases (SEIMC). *Enferm*
669   *Infecc Microbiol Clin* **33**: 626–632.

670   Hair PS, Echague CG, Sholl AM, Watkins JA, Geoghegan JA, Foster TJ, Cunnion KM. 2010.
671   Clumping Factor A Interaction with Complement Factor I Increases C3b Cleavage on the
672   Bacterial Surface of *Staphylococcus aureus* and Decreases Complement-Mediated
673   Phagocytosis. *Infect Immun* **78**: 1717–1727.

674   Higgins J, Loughman A, van Kessel KPM, van Strijp JAG, Foster TJ. 2006. Clumping factor A of
675   *Staphylococcus aureus* inhibits phagocytosis by human polymorphonuclear leucocytes.
676   *FEMS Microbiol Lett* **258**: 290–296.

677   Jolley KA, Bray JE, Maiden MCJ. 2018. Open-access bacterial population genomics: BIGSdb
678   software, the PubMLST.org website and their applications. *Wellcome Open Res* **3**: 124.

679   Kangro K, Wolberg AS, Flick MJ. 2022. Fibrinogen, Fibrin, and Fibrin Degradation Products in
680   COVID-19. *Curr Drug Targets* **23**: 1593–1602.

681   Kaya H, Hasman H, Larsen J, Stegger M, Johannesen TB, Allesøe RL, Lemvigh CK, Aarestrup FM,
682   Lund O, Larsen AR. 2018. SCCmecFinder, a Web-Based Tool for Typing of Staphylococcal
683   Cassette Chromosome *mec* in *Staphylococcus aureus* Using Whole-Genome Sequence
684   Data. *mSphere* **3**: e00612-17.

685 Kern WV, Rieg S. 2020. Burden of bacterial bloodstream infection-a brief update on
686   epidemiology and significance of multidrug-resistant pathogens. *Clin Microbiol Infect*
687   **26**: 151–157.

688 Khatib R, Johnson LB, Fakih MG, Riederer K, Khosrovaneh A, Shamse Tabriz M, Sharma M, Saeed
689   S. 2006. Persistence in *Staphylococcus aureus* bacteremia: incidence, characteristics of
690   patients and outcome. *Scand J Infect Dis* **38**: 7–14.

691 Krueger F. 2012. TrimGalore: A wrapper tool around Cutadapt and FastQC to consistently apply
692   quality and adapter trimming to FastQ files, with some extra functionality for MspI-
693   digested RRBS-type (Reduced Representation Bisufite-Seq) libraries.

694 Lacey KA, Mulcahy ME, Towell AM, Geoghegan JA, McLoughlin RM. 2019. Clumping factor B is
695   an important virulence factor during *Staphylococcus aureus* skin infection and a
696   promising vaccine target. *PLoS Pathog* **15**: e1007713.

697 Larsen MV, Cosentino S, Rasmussen S, Friis C, Hasman H, Marvig RL, Jelsbak L, Sicheritz-Pontén
698   T, Ussery DW, Aarestrup FM, et al. 2012. Multilocus sequence typing of total-genome-
699   sequenced bacteria. *J Clin Microbiol* **50**: 1355–1361.

700 Lee AS, de Lencastre H, Garau J, Kluytmans J, Malhotra-Kumar S, Peschel A, Harbarth S. 2018.
701   Methicillin-resistant *Staphylococcus aureus*. *Nat Rev Dis Primers* **4**: 18033.

702 Liu B, Zheng D, Jin Q, Chen L, Yang J. 2019. VFDB 2019: a comparative pathogenomic platform
703   with an interactive web interface. *Nucleic Acids Res* **47**: D687–D692.

704 Mama OM, Aspiroz C, Ruiz-Ripa L, Ceballos S, Iñiguez-Barrio M, Cercenado E, Azcona JM, López-
705   Cerero L, Seral C, López-Calleja AI, et al. 2021. Prevalence and Genetic Characteristics of
706   *Staphylococcus aureus* CC398 Isolates From Invasive Infections in Spanish Hospitals,
707   Focusing on the Livestock-Independent CC398-MSSA Clade. *Front Microbiol* **12**: 623108.

708 Miller CE, Batra R, Cooper BS, Patel AK, Klein J, Otter JA, Kypraios T, French GL, Tosas O,
709   Edgeworth JD. 2012. An association between bacterial genotype combined with a high-
710   vancomycin minimum inhibitory concentration and risk of endocarditis in methicillin-
711   resistant *Staphylococcus aureus* bloodstream infection. *Clin Infect Dis* **54**: 591–600.

712 Mistry J, Chuguransky S, Williams L, Qureshi M, Salazar GA, Sonnhammer ELL, Tosatto SCE,
713   Paladin L, Raj S, Richardson LJ, et al. 2021. Pfam: The protein families database in 2021.
714   *Nucleic Acids Res* **49**: D412–D419.

715 Monecke S, Coombs G, Shore AC, Coleman DC, Akpaka P, Borg M, Chow H, Ip M, Jatzwauk L,
716   Jonas D, et al. 2011. A field guide to pandemic, epidemic and sporadic clones of
717   methicillin-resistant *Staphylococcus aureus*. *PLoS One* **6**: e17936.

718 Munckhof WJ, Nimmo GR, Carney J, Schooneveldt JM, Huygens F, Inman-Bamber J, Tong E,
719   Morton A, Giffard P. 2008. Methicillin-susceptible, non-multiresistant methicillin-
720   resistant and multiresistant methicillin-resistant *Staphylococcus aureus* infections: a
721   clinical, epidemiological and microbiological comparative study. *Eur J Clin Microbiol*
722   *Infect Dis* **27**: 355–364.

723 Nakaminami H, Ozawa K, Sasai N, Ikeda M, Nemoto O, Baba N, Matsuzaki Y, Sawamura D,
724   Shimoe F, Inaba Y, et al. 2020. Current status of Panton-Valentine leukocidin-positive

725 methicillin-resistant *Staphylococcus aureus* isolated from patients with skin and soft
726 tissue infections in Japan. *J Dermatol* **47**: 1280–1286.

727 Nayfach S, Camargo AP, Schulz F, Eloe-Fadrosh E, Roux S, Kyrpides NC. 2021. CheckV assesses
728 the quality and completeness of metagenome-assembled viral genomes. *Nat Biotechnol*
729 **39**: 578–585.

730 O'Brien L, Kerrigan SW, Kaw G, Hogan M, Penadés J, Litt D, Fitzgerald DJ, Foster TJ, Cox D. 2002.
731 Multiple mechanisms for the activation of human platelet aggregation by
732 *Staphylococcus aureus*: roles for the clumping factors ClfA and ClfB, the serine-aspartate
733 repeat protein SdrE and protein A. *Mol Microbiol* **44**: 1033–1044.

734 Page AJ, Cummins CA, Hunt M, Wong VK, Reuter S, Holden MTG, Fookes M, Falush D, Keane JA,
735 Parkhill J. 2015. Roary: rapid large-scale prokaryote pan genome analysis. *Bioinformatics*
736 **31**: 3691–3693.

737 Park K-H, Greenwood-Quaintance KE, Uhl JR, Cunningham SA, Chia N, Jeraldo PR, Sampathkumar
738 P, Nelson H, Patel R. 2017. Molecular epidemiology of *Staphylococcus aureus*
739 bacteremia in a single large Minnesota medical center in 2015 as assessed using MLST,
740 core genome MLST and spa typing. *PLoS One* **12**: e0179003.

741 Pedruzzi I, Rivoire C, Auchincloss AH, Coudert E, Keller G, de Castro E, Baratin D, Cuche BA,
742 Bougueleret L, Poux S, et al. 2015. HAMAP in 2015: updates to the protein family
743 classification and annotation system. *Nucleic Acids Res* **43**: D1064-1070.

744 Pérez-Montarelo D, Viedma E, Larrosa N, Gómez-González C, Ruiz de Gopegui E, Muñoz-Gallego
745 I, San Juan R, Fernández-Hidalgo N, Almirante B, Chaves F. 2018. Molecular
746 Epidemiology of *Staphylococcus aureus* Bacteremia: Association of Molecular Factors
747 With the Source of Infection. *Front Microbiol* **9**: 2210.

748 Pinchuk IV, Beswick EJ, Reyes VE. 2010. Staphylococcal Enterotoxins. *Toxins (Basel)* **2**: 2177–
749 2197.

750 Raghuram V, Alexander AM, Loo HQ, Petit RA, Goldberg JB, Read TD. 2022. Species-Wide
751 Phylogenomics of the *Staphylococcus aureus* Agr Operon Revealed Convergent
752 Evolution of Frameshift Mutations. *Microbiol Spectr* **10**: e0133421.

753 Rasmussen G, Monecke S, Ehricht R, Söderquist B. 2013. Prevalence of clonal complexes and
754 virulence genes among commensal and invasive *Staphylococcus aureus* isolates in
755 Sweden. *PLoS One* **8**: e77477.

756 Recker M, Laabei M, Toleman MS, Reuter S, Saunderson RB, Blane B, Török ME, Ouadi K, Stevens
757 E, Yokoyama M, et al. 2017. Clonal differences in *Staphylococcus aureus* bacteraemia-
758 associated mortality. *Nat Microbiol* **2**: 1381–1388.

759 Robertson J, Nash JHE. 2018. MOB-suite: software tools for clustering, reconstruction and typing
760 of plasmids from draft assemblies. *Microb Genom* **4**.

761 Sanchez-Herrero JF. 2020. spaTyper.py: Generate spa type identification.
762 https://github.com/HCGB-IGTP/spaTyper (Accessed December 20, 2023).

763 Seemann T. 2017. ABRicate: Mass screening of contigs for antimicrobial resistance or virulence
764 genes. https://github.com/tseemann/abricate (Accessed May 3, 2022).

25

765   Seemann T. 2014. Prokka: rapid prokaryotic genome annotation. *Bioinformatics* **30**: 2068–2069.

766   Seemann T. 2023. Shovill: Assemble bacterial isolate genomes from Illumina paired-end reads.
767   https://github.com/tseemann/shovill (Accessed December 20, 2023).

768   Serra N, Di Carlo P, Andriolo M, Mazzola G, Diprima E, Rea T, Anastasia A, Fasciana TMA, Pipitò
769   L, Capra G, et al. 2023. Staphylococcus aureus and Coagulase-Negative Staphylococci
770   from Bloodstream Infections: Frequency of Occurrence and Antimicrobial Resistance,
771   2018-2021. *Life (Basel)* **13**: 1356.

772   Shohayeb M, El-Banna T, Elsawy LE, El-Bouseary MM. 2023. Panton-Valentine Leukocidin (PVL)
773   genes may not be a reliable marker for community-acquired MRSA in the Dakahlia
774   Governorate, Egypt. *BMC Microbiol* **23**: 315.

775   Sieber RN, Urth TR, Petersen A, Møller CH, Price LB, Skov RL, Larsen AR, Stegger M, Larsen J.
776   2020. Phage-Mediated Immune Evasion and Transmission of Livestock-Associated
777   Methicillin-Resistant *Staphylococcus aureus* in Humans. *Emerg Infect Dis* **26**: 2578–
778   2585.

779   Singer M, Deutschman CS, Seymour CW, Shankar-Hari M, Annane D, Bauer M, Bellomo R,
780   Bernard GR, Chiche J-D, Coopersmith CM, et al. 2016. The Third International Consensus
781   Definitions for Sepsis and Septic Shock (Sepsis-3). *JAMA* **315**: 801.

782   Smith JT, Eckhardt EM, Hansel NB, Eliato TR, Martin IW, Andam CP. 2021. Genomic epidemiology
783   of methicillin-resistant and -susceptible *Staphylococcus aureus* from bloodstream
784   infections. *BMC Infect Dis* **21**: 589.

785   Sterenczak KA, Barrantes I, Stahnke T, Stachs O, Fuellen G, Undre N. 2020. Co-infections: testing
786   macrolides for added benefit in patients with COVID-19. *Lancet Microbe* **1**: e313.

787   Sweet T, Sindi S, Sistrom M. 2023. Going through phages: a computational approach to revealing
788   the role of prophage in *Staphylococcus aureus*. *Access Microbiol* **5**: acmi000424.

789   Uhlemann A-C, McAdam PR, Sullivan SB, Knox JR, Khiabanian H, Rabadan R, Davies PR, Fitzgerald
790   JR, Lowy FD. 2017. Evolutionary Dynamics of Pandemic Methicillin-Sensitive
791   *Staphylococcus aureus* ST398 and Its International Spread via Routes of Human
792   Migration. *mBio* **8**: e01375-16.

793   van der Mee-Marquet N, Dos Santos S, Diene SM, Duflot I, Mereghetti L, Valentin A-S, François
794   P, On Behalf Of The Spiadi Collaborative Group. 2022. Strong Biofilm Formation and Low
795   Cloxacillin Susceptibility in Biofilm-Growing CC398 *Staphylococcus aureus* Responsible
796   for Bacteremia in French Intensive Care Units, 2021. *Microorganisms* **10**: 1857.

797   van Hal SJ, Jensen SO, Vaska VL, Espedido BA, Paterson DL, Gosbell IB. 2012. Predictors of
798   mortality in *Staphylococcus aureus* Bacteremia. *Clin Microbiol Rev* **25**: 362–386.

799   Vázquez-Sánchez DA, Grillo S, Carrera-Salinas A, González-Díaz A, Cuervo G, Grau I, Camoez M,
800   Martí S, Berbel D, Tubau F, et al. 2022. Molecular Epidemiology, Antimicrobial
801   Susceptibility, and Clinical Features of Methicillin-Resistant *Staphylococcus aureus*
802   Bloodstream Infections over 30 Years in Barcelona, Spain (1990-2019). *Microorganisms*
803   **10**: 2401.

804   Viscoli C. 2016. Bloodstream Infections: The peak of the iceberg. *Virulence* **7**: 248–251.

805 Wiggers JB, Xiong W, Daneman N. 2016. Sending repeat cultures: is there a role in the
806   management of bacteremic episodes? (SCRIBE study). *BMC Infect Dis* **16**: 286.

807 Wójcik-Bojek U, Różalska B, Sadowska B. 2022. *Staphylococcus aureus*-A Known Opponent
808   against Host Defense Mechanisms and Vaccine Development-Do We Still Have a Chance
809   to Win? *Int J Mol Sci* **23**: 948.

810 Yilmaz M, Elaldi N, Balkan İİ, Arslan F, Batırel AA, Bakıcı MZ, Gozel MG, Alkan S, Çelik AD, Yetkin
811   MA, et al. 2016. Mortality predictors of *Staphylococcus aureus* bacteremia: a
812   prospective multicenter study. *Ann Clin Microbiol Antimicrob* **15**: 7.

813 Yu J, Gerber GF, Chen H, Yuan X, Chaturvedi S, Braunstein EM, Brodsky RA. 2022. Complement
814   dysregulation is associated with severe COVID-19 illness. *Haematologica* **107**: 1095–
815   1105.

816 Zhang Y, Wu M, Hang T, Wang C, Yang Y, Pan W, Zang J, Zhang M, Zhang X. 2017. *Staphylococcus
817   aureus* SdrE captures complement factor H's C-terminus via a novel 'close, dock, lock
818   and latch' mechanism for complement evasion. *Biochem J* **474**: 1619–1631.

819